

REPORT DOCUMENTATION PAGE

AD-A214 554

1b. RESTRICTIVE MARKINGS

none

3. DISTRIBUTION/AVAILABILITY OF REPORT

Distribution unlimited

2b. DECLASSIFICATION/DOWNGRADING SCHEDULE

4. PERFORMING ORGANIZATION REPORT NUMBER(S)

SBIL - A89

5. MONITORING ORGANIZATION REPORT NUMBER(S)

6a. NAME OF PERFORMING ORGANIZATION

State University of New York

6b. OFFICE SYMBOL
(If applicable)

7a. NAME OF MONITORING ORGANIZATION

Office of Naval Research

6c. ADDRESS (City, State and ZIP Code)

Chemistry Department
SUNY
Stony Brook, NY 11794-3400

7b. ADDRESS (City, State and ZIP Code)

Code 1132
800 N. Quincy Street
Arlington, VA 222178a. NAME OF FUNDING/SPONSORING
ORGANIZATION

ONR

8b. OFFICE SYMBOL
(If applicable)

9. PROCUREMENT INSTRUMENT IDENTIFICATION NUMBER

N00014-85K-00678

8c. ADDRESS (City, State and ZIP Code)

Code 1132
800 N. Quincy Street
Arlington, VA 22217

10. SOURCE OF FUNDING NOS

PROGRAM
ELEMENT NO.PROJECT
NO.TASK
NO.WORK UNIT
NO.

11. TITLE (Include Security Classification)

See Title Page

12. PERSONAL AUTHOR(S)

P.A. Hintz, S.A. Ruatta, S.L. Anderson

13a. TYPE OF REPORT

interim

13b. TIME COVERED

FROM TO

14. DATE OF REPORT (Yr., Mo., Day)

1989, October, 28

15. PAGE COUNT

26

16. SUPPLEMENTARY NOTATION

17. COSATI CODES

FIELD GROUP SUB GR

18. SUBJECT TERMS (Continue on reverse if necessary and identify by block number)

Boron Combustion, Clusters, Propulsion

19. ABSTRACT (Continue on reverse if necessary and identify by block number)

We report reaction probabilities for surface reactions of boron with various gases as a function of temperature. These kinetic parameters are based on averages of cross sections measured for reactions of boron cluster ions with the gases in question. We present both total reaction probabilities and also the branching fractions to different products. The method for converting from cross sections to rates is discussed and results are given for reaction with oxygen, hydrogen, nitrogen, nitrous oxide, water methane, fluoromethane, carbon dioxide, carbon monoxide, and silane. K

S ELECT **D**
NOV 15 1989
B

20. DISTRIBUTION/AVAILABILITY OF ABSTRACT

UNCLASSIFIED/UNLIMITED ☒ SAME AS RPT. ☐ DTIC USERS ☐

21. ABSTRACT SECURITY CLASSIFICATION

None

22a. NAME OF RESPONSIBLE INDIVIDUAL

Gabriel Roy

22b. TELEPHONE NUMBER

(Include Area Code)
202-696-4403

22c. OFFICE SYMBOL

DD FORM 1473, 83 APR

EDITION OF 1 JAN 73 IS OBSOLETE.

unclassified

SECURITY CLASSIFICATION OF THIS PAGE

DISTRIBUTION STATEMENT A

Approved for public release;
Distribution Unlimited

89 11 13 104

Cluster Based Reaction Probabilities for Boron with
Oxygen, Hydrogen, Water, Nitrogen, Nitrous Oxide,
Carbon Dioxide, Carbon Monoxide, Methane,
Tetrafluoromethane, and Silane

Paul A. Hintz, Stephen A. Ruatta, and Scott L. Anderson
Department of Chemistry
State University of New York at Stony Brook
Stony Brook, NY 11794-3400

I Introduction

Since we have begun our detailed study of boron cluster ion reaction dynamics, we have tried to present our cross section measurements in a form most useful to combustion modelers and others interested in the reactivity of boron, and in oxidation processes in particular. An effective way we have found to do this is to convert our data into "reaction efficiencies" or the probability of reaction per surface collision. By calculating these reaction probabilities as a function of temperature, we can provide combustion modelers with the necessary data to calculate reaction rates for boron combustion processes under whatever conditions seem appropriate. Our reaction studies have focused on oxidation reactions of boron cluster ions with O_2 , D_2O , CO_2 , CO , and N_2O . We have studied various other neutral reactant gases including CH_4 , CF_4 , D_2 , N_2 , and SiH_4 . Our goal is to build a comprehensive picture of boron cluster ion reactivity. This report contains reaction efficiency data for all reaction systems studied to date.

II. Calculation Method

In order to estimate the reaction efficiency of the reaction of boron clusters ions with neutral gases, the probability of reaction per collision at a given energy is averaged over a Boltzmann energy distribution to yield a reaction probability at various temperatures. The experimental cross section data for the major products of the reactions of two representative cluster ions (B_6^+ and B_{12}^+) with N_2 , N_2O , CO , CO_2 , CH_4 , CF_4 , SiH_4 , D_2 , D_2O , and O_2 are shown in Figures 1 and 2. Notice the extensive variation in the magnitude and shape of the cross sections for the different reactions. In some cases, the reaction proceeds with no activation energy (ie. reactivity peaks at low collision energy) but in other cases, significant activation barriers are observed, even though the overall reactions are in most cases exothermic.

To estimate the reaction probability per collision, we compare the experimental cross sections (σ_{exp}) from 0 to 10 eV collision energy (center of mass) with the collision cross section which can be estimated with reasonable certainty. For this study, the collision cross section is given by the locked ion-dipole capture cross section:

$$\sigma_{lock} = \sigma_{lang} + (C * \sigma_{dip}).$$

σ_{lang} is the Langevin polarization capture cross section defined as:

$$\sigma_{lang} = 16.859 * (\alpha/E(eV))^{1/2},$$

where α is the polarizability of the neutral reactant. σ_{dip} is the ion-dipole capture cross section defined as:

$$\sigma_{dip} = 9.4186 * D(\text{debye}) / E(eV),$$

where D is the dipole moment of the reactant gas. C is the locking constant for the,

Availability Co

Dist	Avail and/or Special
------	----------------------

A-1	
-----	--

locked dipole approximation ($C = 0.318$ for this study). When the reactant gas molecule has no dipole moment, σ_{lang} was used. This form of the collision cross section is used at low collision energies. At high energies, capture effects become less important and the collision cross section is given instead by the physical size (hard sphere cross section) of the reactants. The hard sphere cross section is given by:

$$\sigma_{\text{hs}} = \pi * (R_c + R_g)^2,$$

where R_c is the radius of the cluster and R_g is the radius of the neutral gas molecule.

The reaction efficiency is thus given by the ratio: $\sigma_{\text{exp}}/\sigma_{\text{col}}$ where σ_{col} is the larger of σ_{lock} or σ_{hs} . This ratio provides an estimate of the absolute reactivity of these systems at various collision energies. In order to calculate the reaction probability at various temperatures of the reaction, these ratios are averaged over a Maxwell-Boltzmann distribution. These distributions are of the form:

$$dn = 2\pi N[\pi kT]^{-3/2} \epsilon^{1/2} e^{-\epsilon/kT} d\epsilon.$$

Several of these distributions at various temperatures are shown in Figure 3. Note that the maxima of these distributions occur at very low energies (< 0.1 eV). The distributions are normalized so that the area under the curves equal 1. The integral of the reactivity at a specific energy times the corresponding Boltzmann factor yields a reaction probability or "efficiency" at a specific temperature. This calculation was done for temperatures between 300 and 2500 K.

III. Results

The results are compiled in Tables 1 and 2. We give total reaction efficiency as

a function of temperature as well as the efficiencies for formation of all the major products. All values lie between 0 and 1 where 1 represents the maximum reaction efficiency. The data in Tables 1 and 2 are plotted in Figures 4-13. In general, the reaction probabilities for most of the reaction systems studied tend to increase with increasing temperature and then level off or decrease slightly.

The reactions which preferentially form oxide products are those with O_2 and CO_2 . The reaction efficiencies for these reactions are plotted versus temperature in Figures 4 and 5. Oxide formation makes up a significant percentage of the total reaction probability for the O_2 reactions and the majority for the CO_2 reactions. B_6^+ is much more efficient at forming oxides than B_{12}^+ however. N_2O reactions also result in oxide formation (Figure 6) but for some smaller clusters such as B_6^+ , the largest percentage of the reaction probability is due to boron-nitride formation. The larger clusters, which should be more representative of bulk boron surfaces, react preferentially to form oxide products by a factor of 4. Some nitride is produced however and we believe that reactions with NO_x species is the likely source of the BN solid observed by Kuo and co-workers in boron fuel combustion. Reactions with D_2O (Figure 7) lead to only a small amount of oxide formation for the small size clusters (six atoms and less) while the reaction efficiency for the large cluster oxide formation is zero. The formation of the hydride is the largest percentage of the reaction probability for most cluster sizes. Almost the entire reaction probability for the CO reactions (Figure 8) is due to the adduct formation at very low collision energies (< 0.2 eV). No reactive oxide formation is detected. The reaction probability for other neutral gases varies considerably. N_2

(Figure 9) is very nonreactive with reaction efficiencies in the millionth of a percent range at 2500 K. D_2 reactions (Figure 10) yield significant reaction efficiencies but these are considerably temperature dependant, especially for B_{12}^+ . The efficiencies for the reaction of methane and boron cluster ions is very dependent on cluster size (Figure 11). For B_6^+ , the total reaction probability is near unity and nearly constant with temperature. The reaction probability for B_{12}^+ is an order of magnitude smaller and is much more temperature dependant. Figure 12 shows the reaction probability for the reaction of B_6^+ with CF_4 . The products formed are quite different than those of the analogous methane reactions, forming fluorides over carbides. The reaction probability for fluoride formation is only about 40% and is quite temperature dependant. The reaction of B_{12}^+ with CF_4 was not studied. The results for the reactions with silane (Figure 13) are quite similar for both B_6^+ and B_{12}^+ with addition of SiH_n ($n = 0-3$) to the intact cluster making up over 90% of the total reaction probability. The temperature dependence is also similar for both cluster sizes. In Figures 14 and 15, the total reaction probabilities versus temperature for the various reactions of neutral gases with B_6^+ and B_{12}^+ respectively are shown. Methane, silane, water and carbon dioxide have the largest total reaction efficiencies for reactions with B_6^+ while silane, water and nitrous oxide are largest for B_{12}^+ . For the majority of the reactions with B_{12}^+ , the total reaction efficiencies are less than 10% while for B_6^+ , all the totals except for N_2 , are greater than 10% of the maximum reaction efficiency.

For most of these reactions, we have only surveyed the chemistry for B_6^+ and B_{12}^+ . Based on more detailed studies of all size clusters reacting with O_2 , D_2 , D_2O , CO_2 and

N_2O , we believe that B_{12}^+ is quite representative of the chemistry of large clusters. Further studies are in progress of the detailed chemistry with these and other reactants. In addition, we are preparing to carry out studies of much larger clusters.

TEMPERATURE (K)

PRODUCTS	300	750	1000	1250	1500	1750	2000	2250	2500
B6+ + N2									
B+	5.2E-39	3.0E-18	8.8E-15	1.1E-12	2.7E-11	0.000000	0.000000	0.000000	0.000000
B3N+	6.8E-78	4.0E-33	9.4E-26	2.3E-21	1.9E-18	2.3E-16	8.1E-15	1.3E-13	1.2E-12
B4N2+	2.3E-39	1.4E-18	3.9E-15	4.8E-13	1.2E-11	1.2E-10	0.000000	0.000000	0.000000
TOTALS	7.5E-39	4.4E-18	1.3E-14	1.6E-12	3.9E-11	0.000000	0.000000	0.000000	0.000000
B6+ + N2O									
B5+	0.046511	0.079841	0.094906	0.107944	0.119094	0.128550	0.136542	0.143298	0.149026
B5N+	0.037874	0.055335	0.060415	0.063558	0.065344	0.066181	0.066356	0.066073	0.065472
B6N+	0.134031	0.240353	0.279334	0.308705	0.330829	0.347440	0.359833	0.368981	0.375626
B6O+	0.054669	0.086368	0.096071	0.102304	0.106075	0.108092	0.108860	0.108739	0.107986
OTHER	0.034274	0.047104	0.051019	0.053587	0.055156	0.055988	0.056280	0.056183	0.055809
TOTAL	0.307360	0.509003	0.581747	0.636100	0.676499	0.706253	0.727873	0.743275	0.753921
B6+ + CO									
B+	0.000165	0.000213	0.000221	0.000223	0.000221	0.000218	0.000215	0.000212	0.000209
B5+	0.003270	0.008209	0.010546	0.012617	0.014432	0.016007	0.017367	0.018539	0.019549
B6CO+	0.348308	0.414467	0.417357	0.409034	0.394380	0.376549	0.357491	0.338354	0.319784
TOTAL	0.351744	0.422910	0.428125	0.421875	0.409034	0.392776	0.375074	0.357106	0.339542
B6+ + CO2									
B6O+	0.618988	0.735733	0.764272	0.779332	0.784651	0.783080	0.776744	0.767190	0.755529
B6O2+	0.126479	0.138505	0.137985	0.135262	0.131201	0.126404	0.121268	0.116046	0.110894
OTHER	0.012784	0.021224	0.023814	0.025459	0.026441	0.026963	0.027170	0.027172	0.027047
TOTAL	0.757876	0.882305	0.904897	0.913566	0.912874	0.905762	0.894302	0.879986	0.863890
B6+ + CH4									
B4CHN+	0.000439	0.000610	0.000715	0.000821	0.000921	0.001013	0.001094	0.001166	0.001230
B5CHn+	0.010003	0.019316	0.021203	0.021831	0.021777	0.021390	0.020868	0.020314	0.019782
B6CHn+	0.908414	0.971642	0.979751	0.982737	0.982025	0.977989	0.970939	0.961305	0.949597
OTHER	0.000058	0.000073	0.000078	0.000084	0.000090	0.000096	0.000104	0.000112	0.000120
TOTAL	0.909274	0.971929	0.979969	0.982983	0.982406	0.978615	0.971906	0.962692	0.951460
B6+ + CF4									
CF3+	0.055111	0.079358	0.096070	0.112775	0.128040	0.141225	0.152213	0.161161	0.168340
B6F+	0.111285	0.094814	0.093431	0.095443	0.098878	0.102646	0.106207	0.109327	0.111936
B6F2+	0.034359	0.060995	0.068743	0.073395	0.075940	0.077045	0.077163	0.076607	0.075591
OTHER	0.029831	0.042792	0.047069	0.050035	0.051999	0.053195	0.053809	0.053984	0.053831
TOTAL	0.230587	0.277961	0.305316	0.331650	0.354858	0.374112	0.389394	0.401081	0.409700
B6+ + SiH4									
SiHn+	0.000188	0.000651	0.000957	0.001298	0.001677	0.002097	0.002562	0.003079	0.003654
B5SiHn+	0.041300	0.059619	0.066902	0.073041	0.078236	0.082607	0.086254	0.089272	0.091751
B6SiHn+	0.420656	0.617482	0.684600	0.734518	0.772616	0.801853	0.824499	0.842046	0.855560
OTHER	0.000036	0.000022	0.000018	0.000019	0.000026	0.000040	0.000062	0.000093	0.000134
TOTAL	0.462125	0.670543	0.736413	0.783191	0.817385	0.842930	0.862303	0.877127	0.888509

Table 1

B6+ + D2

B+	0.000005	0.000130	0.000238	0.000350	0.000459	0.000562	0.000657	0.000745	0.000826
B5+	0.000368	0.001067	0.001426	0.001758	0.002052	0.002302	0.002508	0.002673	0.002804
B5D+	0.001124	0.001531	0.001608	0.001628	0.001615	0.001581	0.001538	0.001489	0.001438
B6D+	0.049419	0.081288	0.094756	0.106027	0.115471	0.123400	0.130078	0.135727	0.140530
B6D2+	0.096182	0.112347	0.109416	0.103996	0.097757	0.091451	0.085415	0.079785	0.074503
TOTAL	0.147100	0.196364	0.207445	0.213761	0.217355	0.219298	0.220197	0.220421	0.220202

B6+ + D2

B40+	0.006865	0.010396	0.011600	0.012462	0.013075	0.013505	0.013802	0.014002	0.014131
B50+	0.006151	0.008642	0.009245	0.009536	0.009627	0.009591	0.009476	0.009312	0.009119
B60+	0.013200	0.019748	0.021913	0.023461	0.024593	0.025444	0.026101	0.026618	0.027033
C10	0.049749	0.076277	0.085718	0.092792	0.098157	0.102277	0.105484	0.108010	0.110024
TOTAL	0.075966	0.115066	0.128477	0.138253	0.145453	0.150819	0.154864	0.157944	0.160308

B6+ + D2C

OTHER	0.064712	0.119499	0.138102	0.151631	0.161754	0.169547	0.175716	0.180742	0.184951
B5D+	0.259666	0.479778	0.555826	0.611372	0.652151	0.681798	0.702815	0.717054	0.725945
B60D+	0.129373	0.239272	0.275968	0.301534	0.319059	0.330666	0.337867	0.341763	0.343175
TOTAL	0.445906	0.727998	0.797565	0.841560	0.871014	0.891413	0.905717	0.915664	0.922356

Table 1 (cont)

TEMPERATURE (K)

PRODUCT	300	750	1000	1250	1500	1750	2000	2250	2500
B12+ + N2									
B11N2+	3.5E-38	1.7E-17	4.3E-14	4.7E-12	1.1E-10	9.8E-10	5.2E-09	1.9E-08	5.2E-08
B12+ + N2O									
B11O+	0.019582	0.027709	0.02918	0.029506	0.029163	0.028452	0.027554	0.026577	0.025583
B12N+	0.024932	0.040716	0.044265	0.045705	0.045857	0.045248	0.044206	0.042933	0.041554
B12O+	0.146261	0.203904	0.214206	0.216312	0.213545	0.208028	0.201071	0.193463	0.185673
OTHER	0.005816	0.008006	0.00838	0.008442	0.008324	0.008106	0.007838	0.007551	0.007261
TOTAL	0.196591	0.280335	0.296031	0.299965	0.296888	0.289834	0.28067	0.270525	0.26007
B12+ + CO									
B+	0.00014	0.000107	0.000108	0.000117	0.000127	0.000137	0.000146	0.000154	0.00016
B12CO+	0.01551	0.018108	0.018121	0.017674	0.016971	0.016148	0.015285	0.014428	0.013602
TOTAL	0.015649	0.018216	0.01823	0.01779	0.017098	0.016285	0.015431	0.014582	0.013763
B12+ + CO2									
B12O+	0.000039	0.000084	0.000135	0.000193	0.000256	0.000321	0.000388	0.000457	0.000528
B12+ + CH4									
B11CHn+	3.5E-06	0.000084	0.00016	0.000239	0.000314	0.000379	0.000432	0.000473	0.000505
B12CHn+	0.014626	0.024738	0.028108	0.030538	0.032353	0.033767	0.034911	0.035871	0.036701
OTHER	0.002101	0.003151	0.004637	0.006343	0.008034	0.009588	0.010956	0.012134	0.013137
TOTAL	0.016731	0.027973	0.032904	0.03712	0.040702	0.043733	0.046298	0.048479	0.050344
B12+ + SiH4									
SiH3+	9.2E-06	0.000022	0.000027	0.000029	0.000031	0.000032	0.000033	0.000034	0.000034
B11SiHn+	0.016347	0.025863	0.028898	0.031004	0.032463	0.033458	0.034117	0.034528	0.034758
B12SiHn+	0.283038	0.463245	0.533613	0.590579	0.636928	0.674569	0.704972	0.729342	0.748678
TOTAL	0.299394	0.488798	0.5613	0.618988	0.665219	0.702319	0.732016	0.755653	0.774302
B12+ + D2									
B11+	7.5E-07	0.000419	0.001249	0.002383	0.003611	0.004783	0.005819	0.006691	0.007398
B12D+	6.7E-08	0.000039	0.000123	0.000252	0.000414	0.0006	0.000802	0.001018	0.001245
B12D2+	0.001852	0.004538	0.005626	0.006644	0.007633	0.008591	0.009509	0.010375	0.011182
TOTAL	0.001853	0.004996	0.006998	0.009279	0.011658	0.013974	0.01613	0.018084	0.019663
B12+ + O2									
B11O+	0.005222	0.007426	0.00797	0.008244	0.008347	0.008334	0.008265	0.008146	0.008001
B1O+	0.021328	0.033725	0.038295	0.041827	0.044635	0.046932	0.048865	0.050535	0.052014
B9+	4.7E-21	2.3E-10	1.4E-08	1.7E-07	9.2E-07	3.1E-06	8.1E-06	0.000017	0.000032
B11+	1.0E-37	6.0E-17	1.7E-13	2.1E-11	5.3E-10	5.3E-09	3.1E-08	1.2E-07	3.6E-07
TOTAL	0.02655	0.041151	0.046265	0.050072	0.052982	0.055275	0.057137	0.058698	0.060048
B12+ + D2O									
B10D2+	0.058072	0.053136	0.046067	0.039964	0.034965	0.030898	0.027565	0.024806	0.022496
B11D+	0.351217	0.46398	0.472338	0.469593	0.461263	0.449861	0.436762	0.422801	0.408516
TOTAL	0.409289	0.517115	0.518405	0.509558	0.496229	0.480759	0.464327	0.447608	0.431011

Table 2

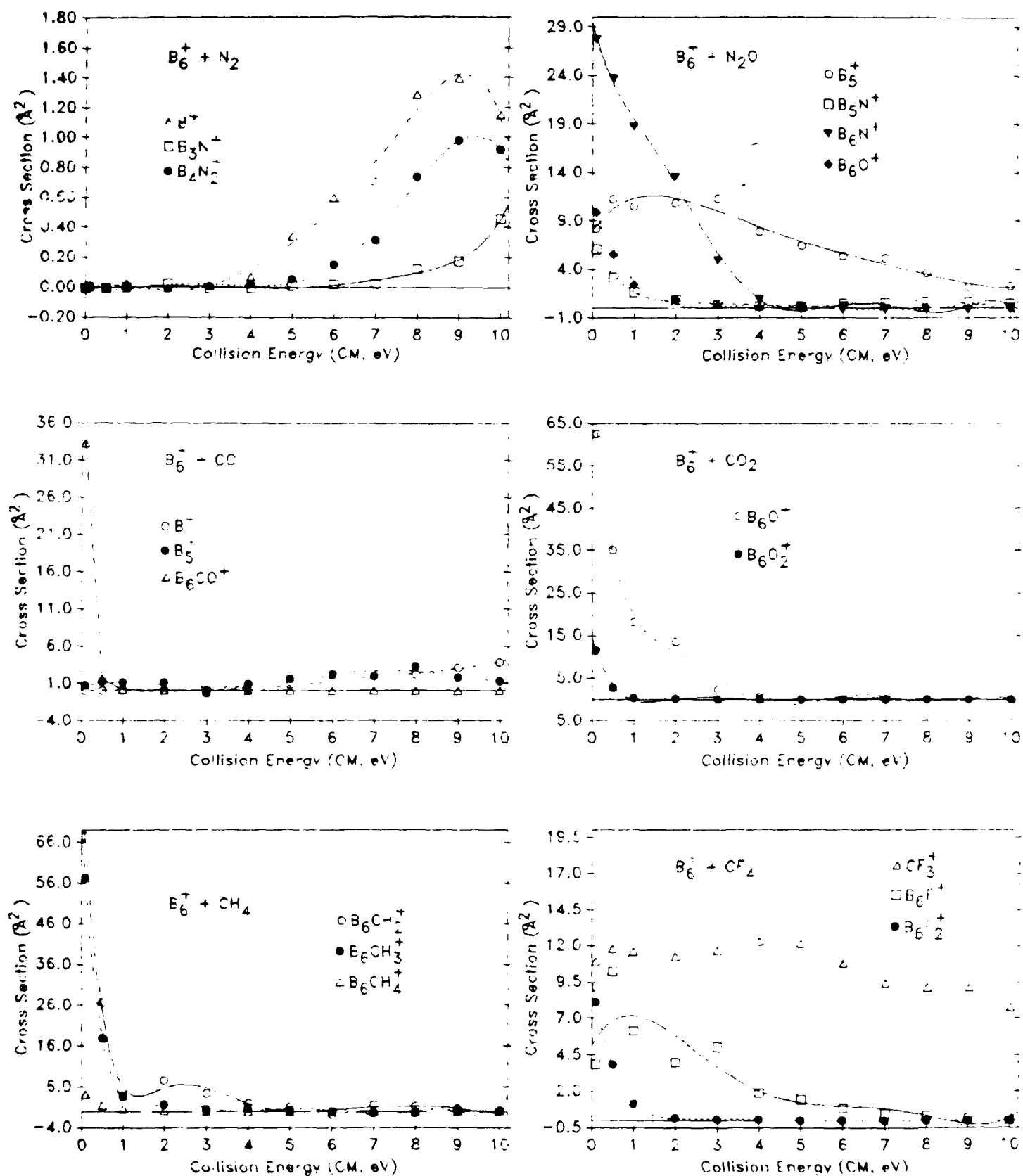


Figure 1(a)

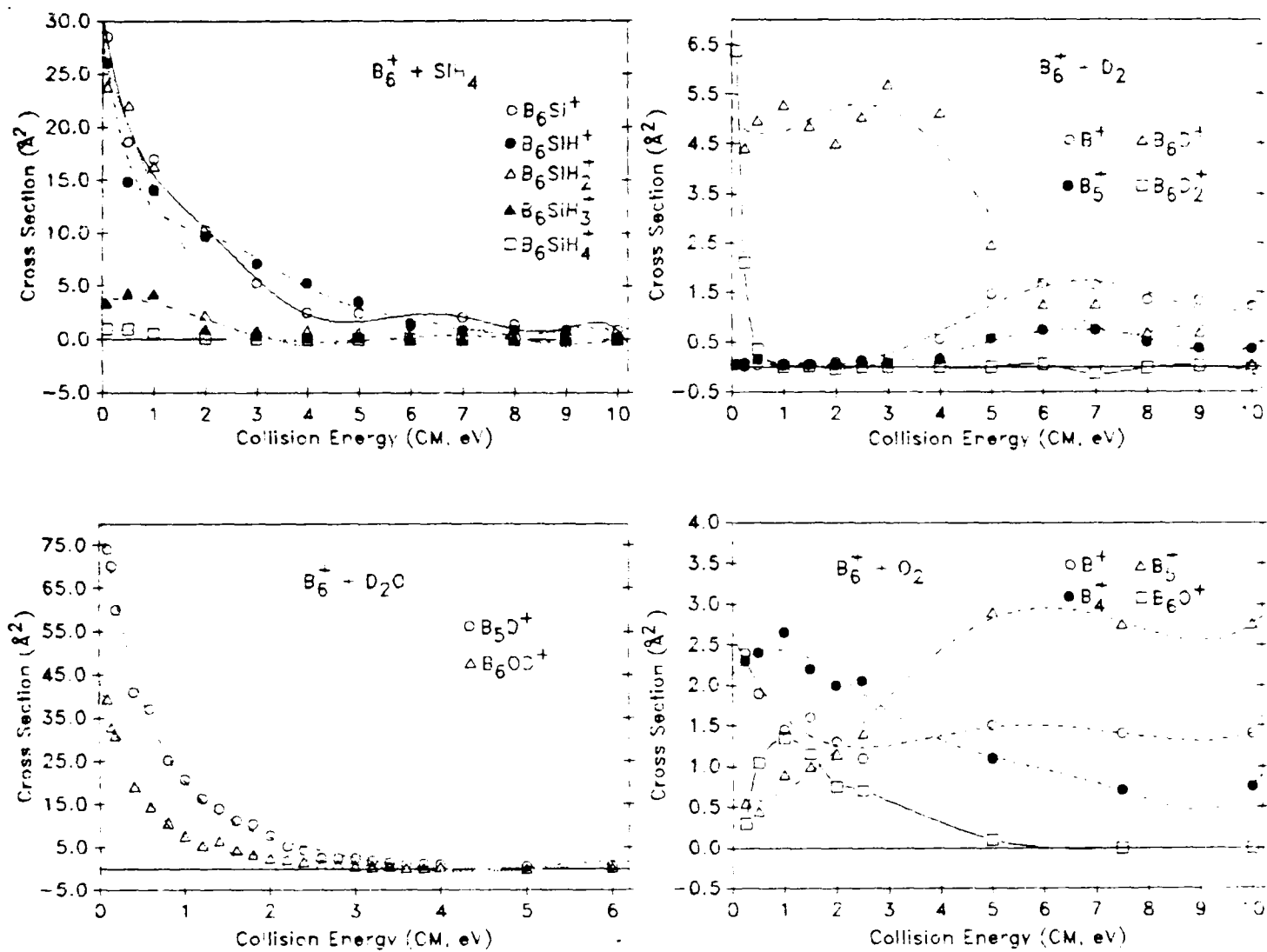


Figure 1(b)

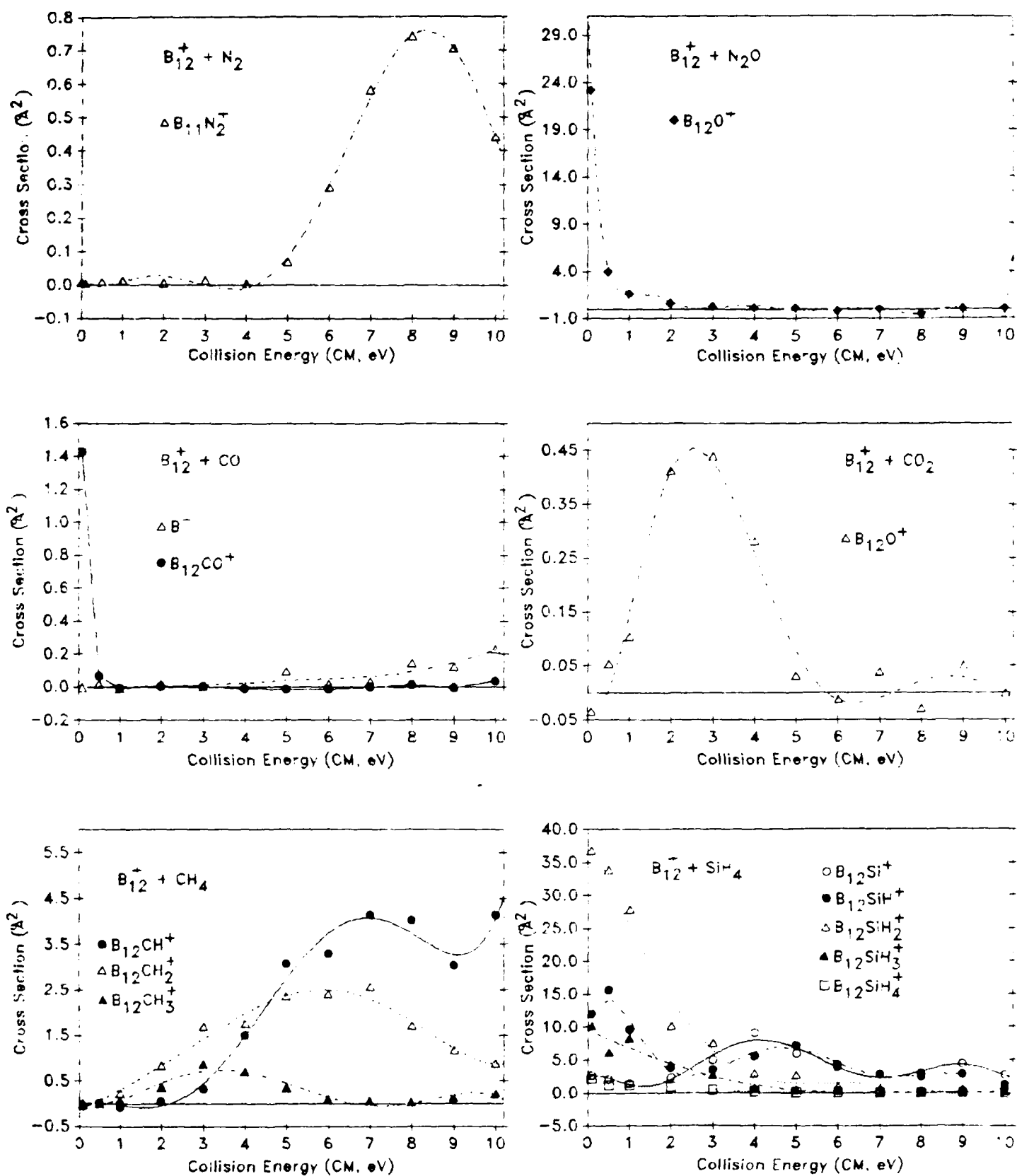


Figure 2(a)

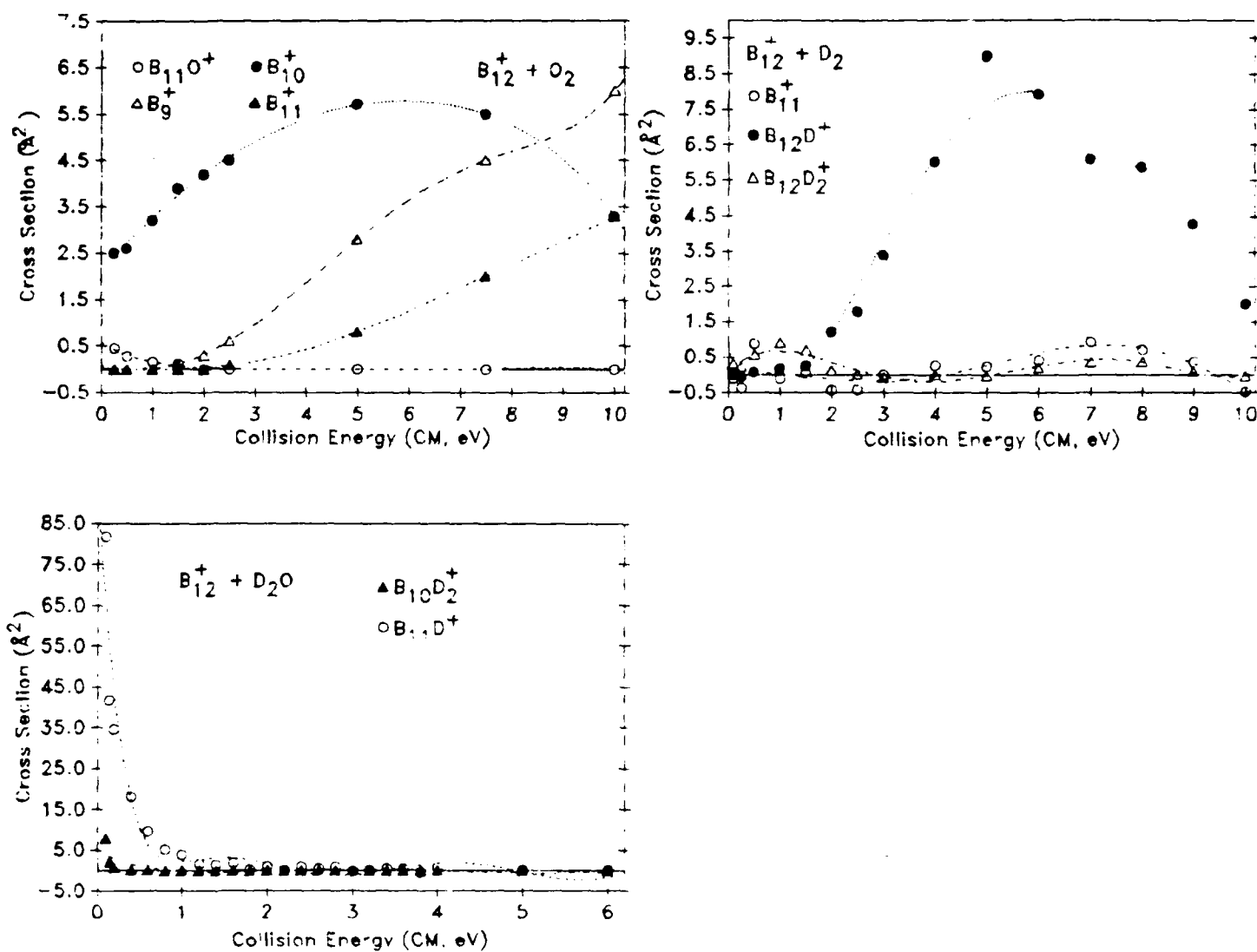


Figure 2(b)

MAXWELL DISTRIBUTION

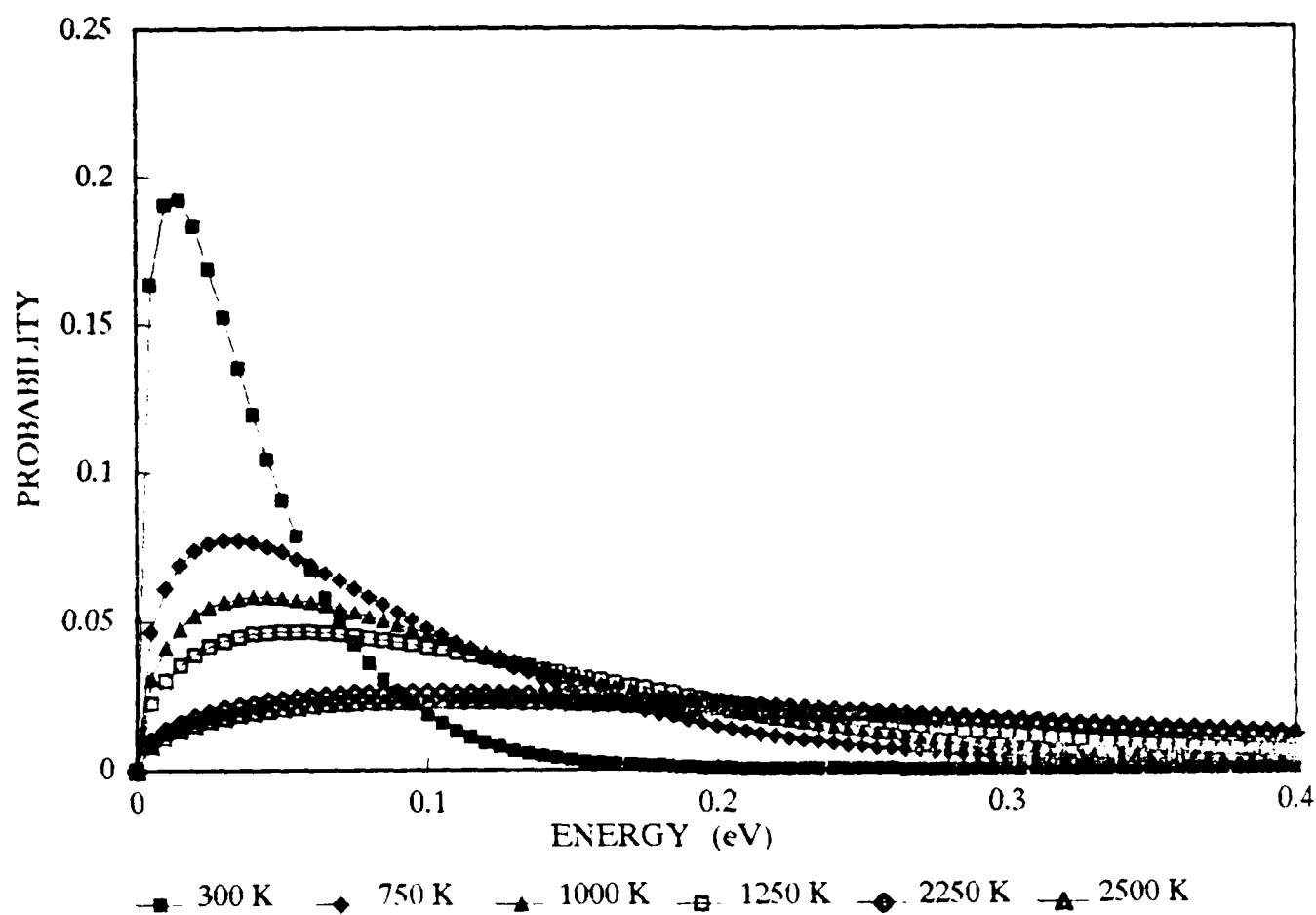


Figure 3

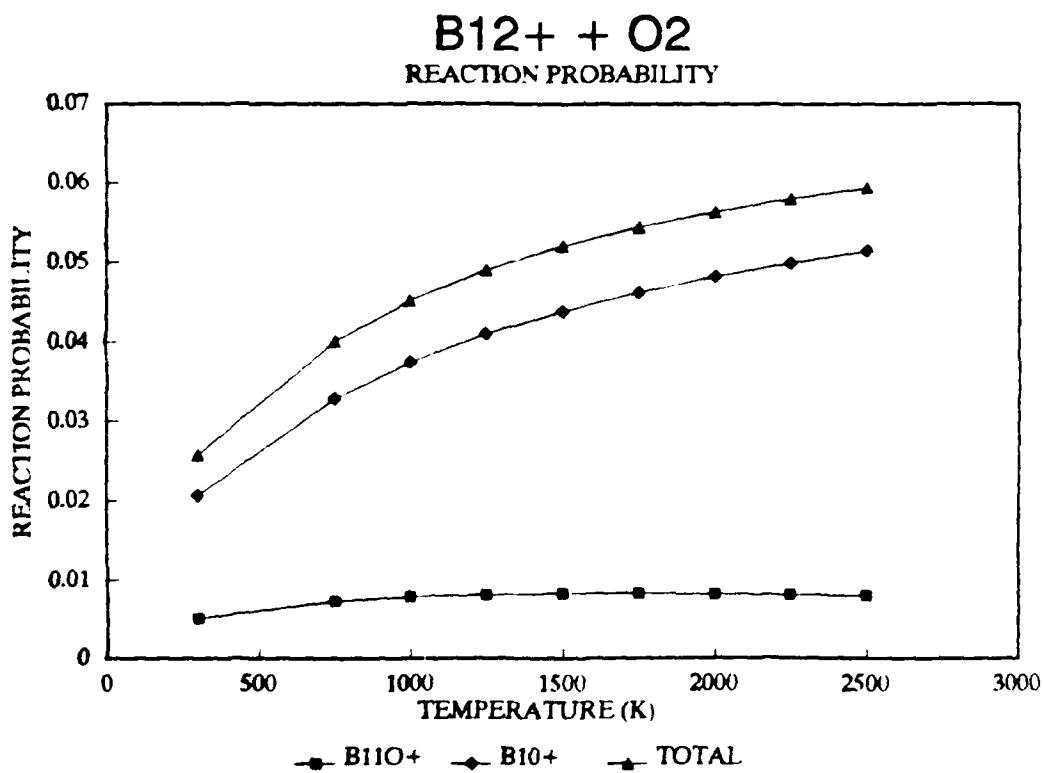
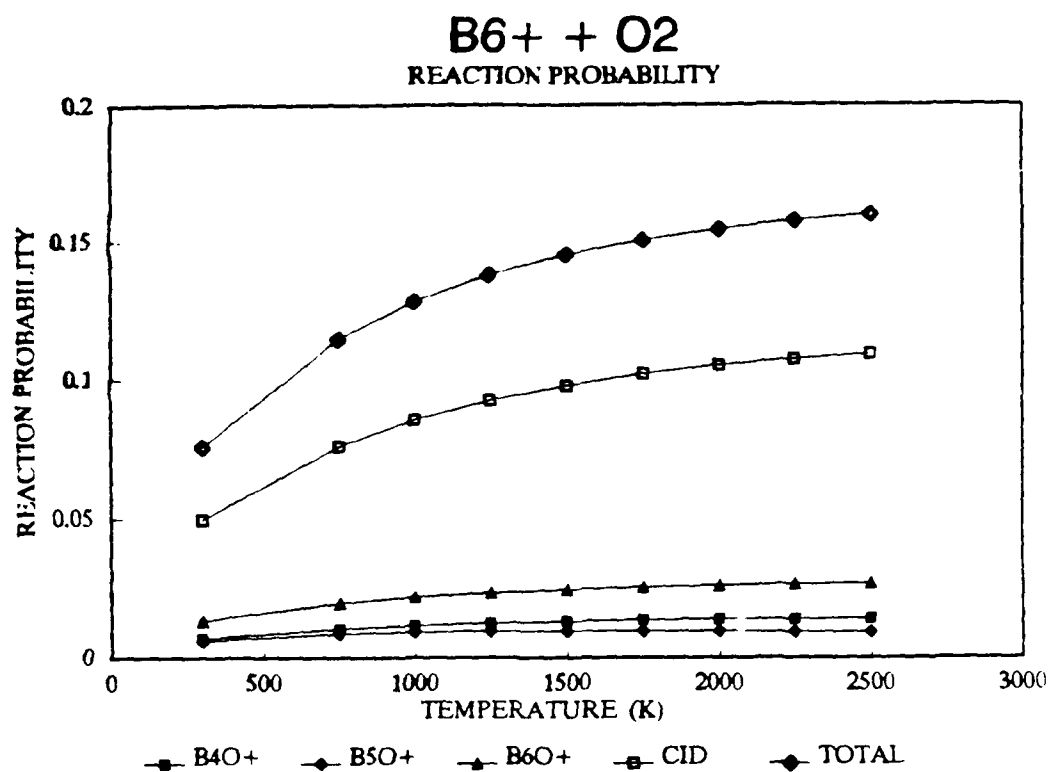


Figure 4

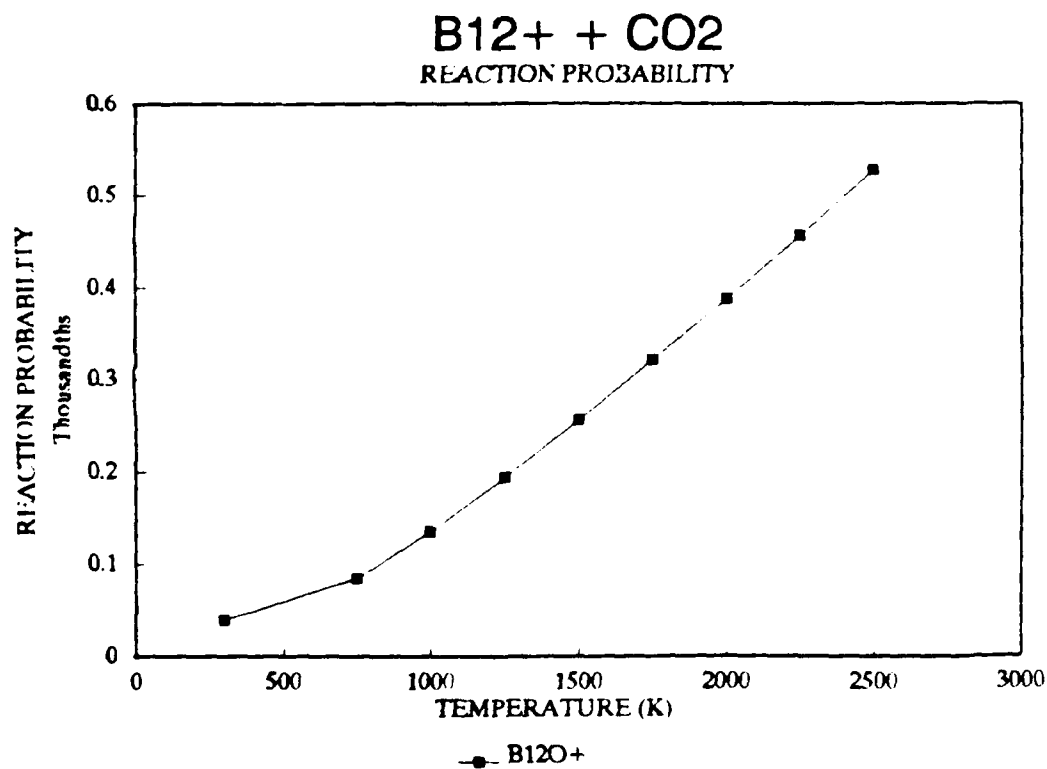
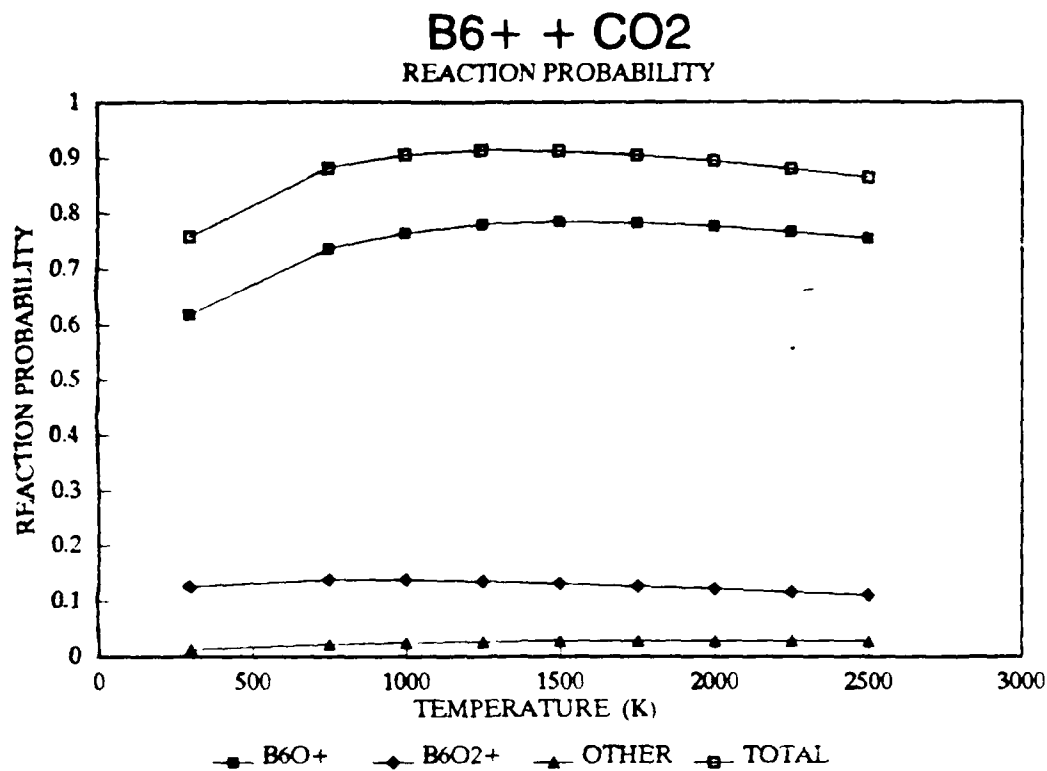


Figure 5

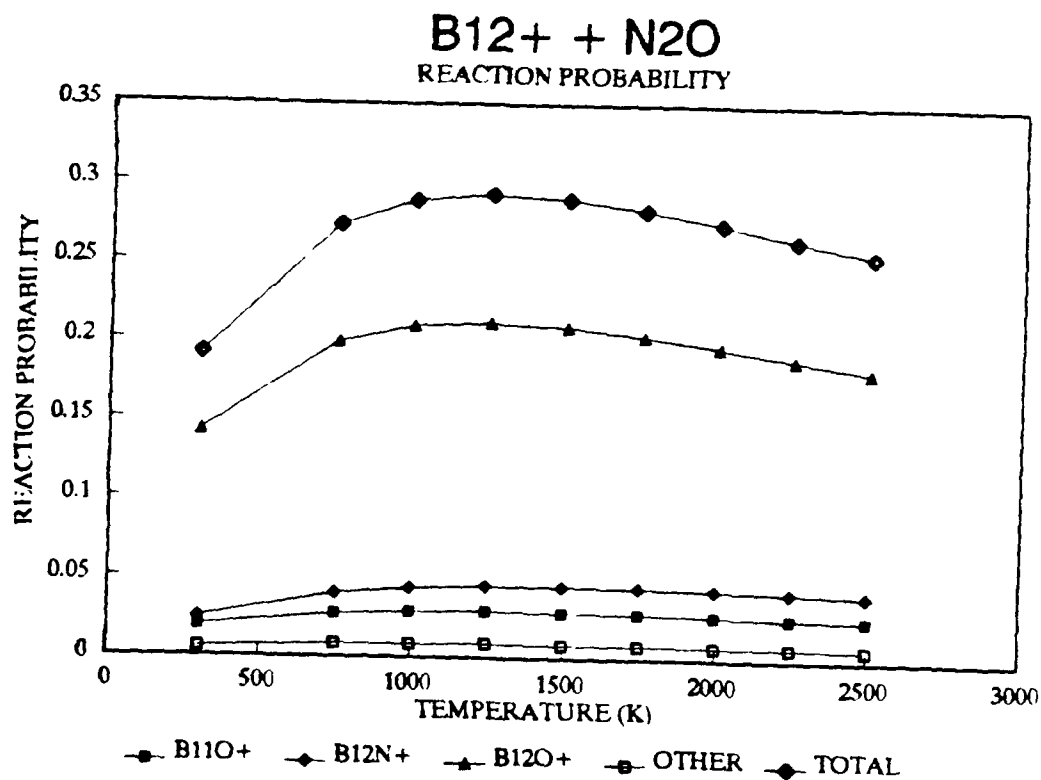
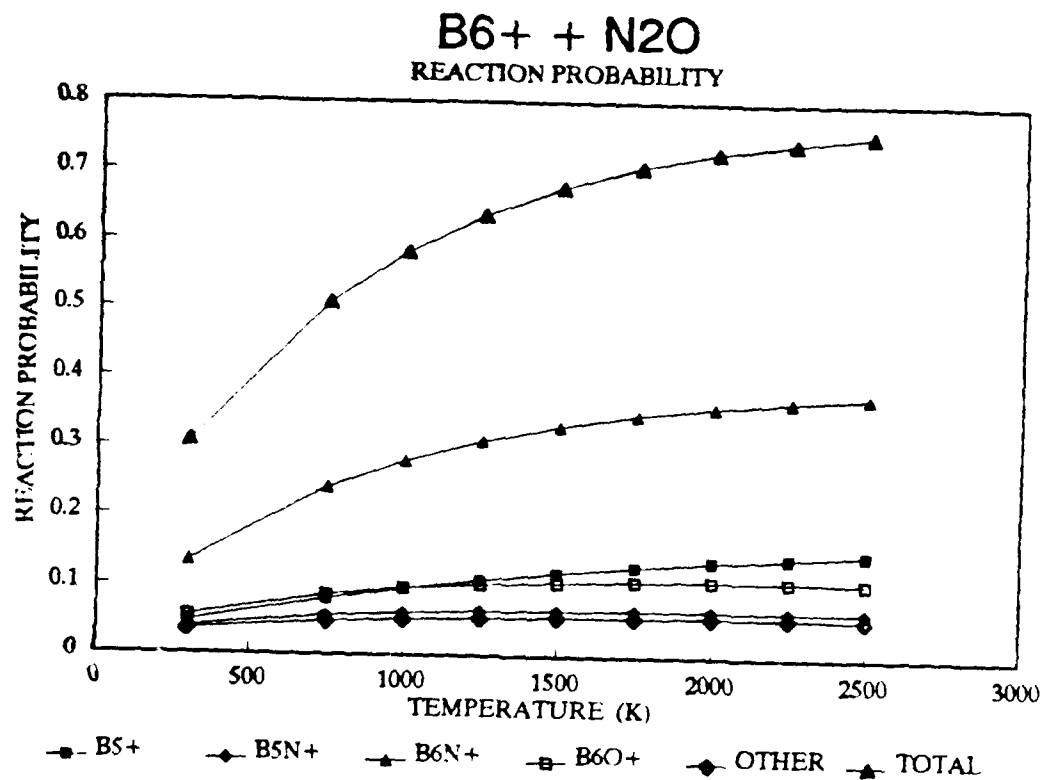


Figure 6

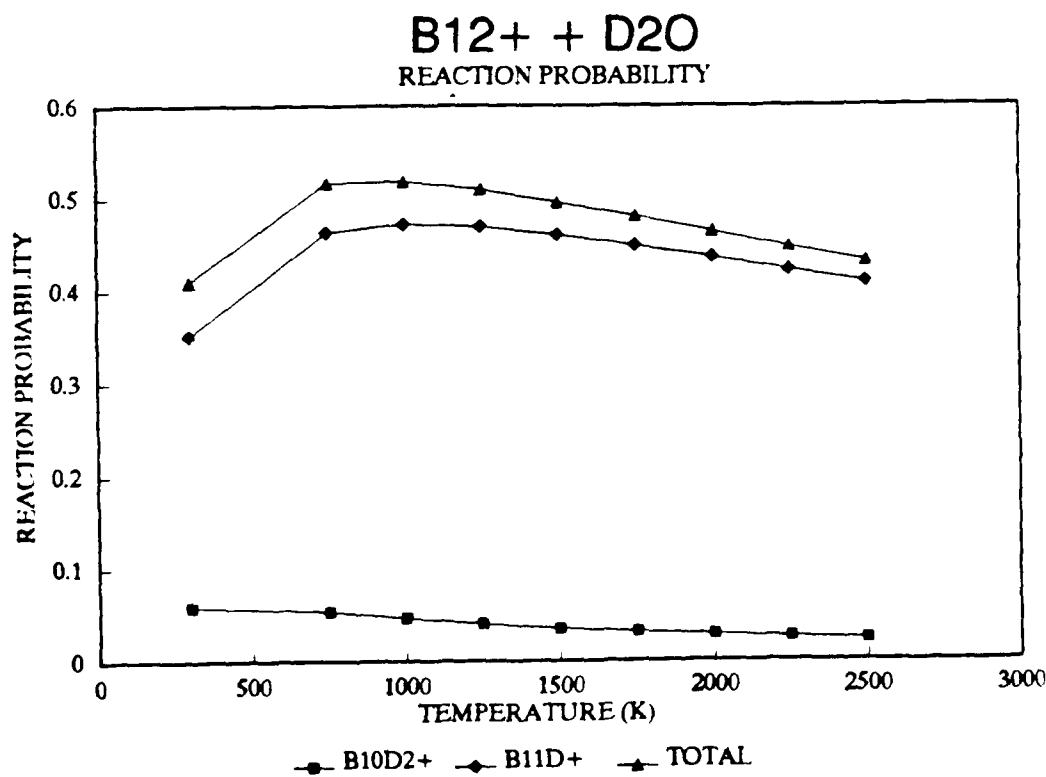
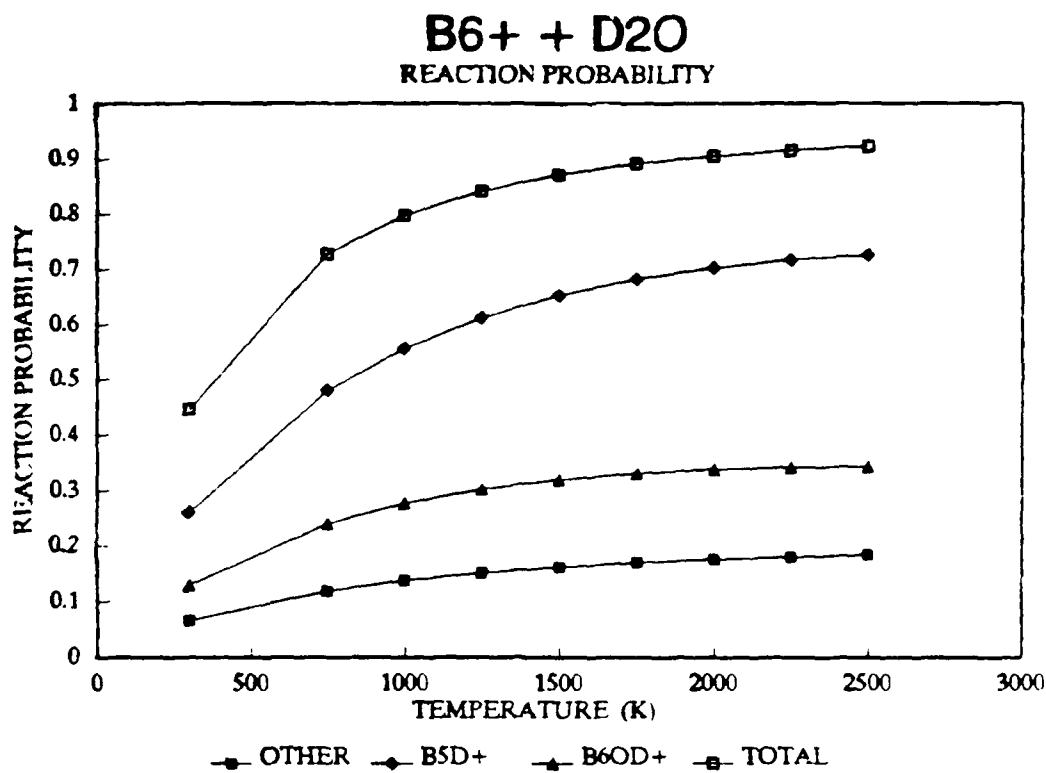


Figure 7

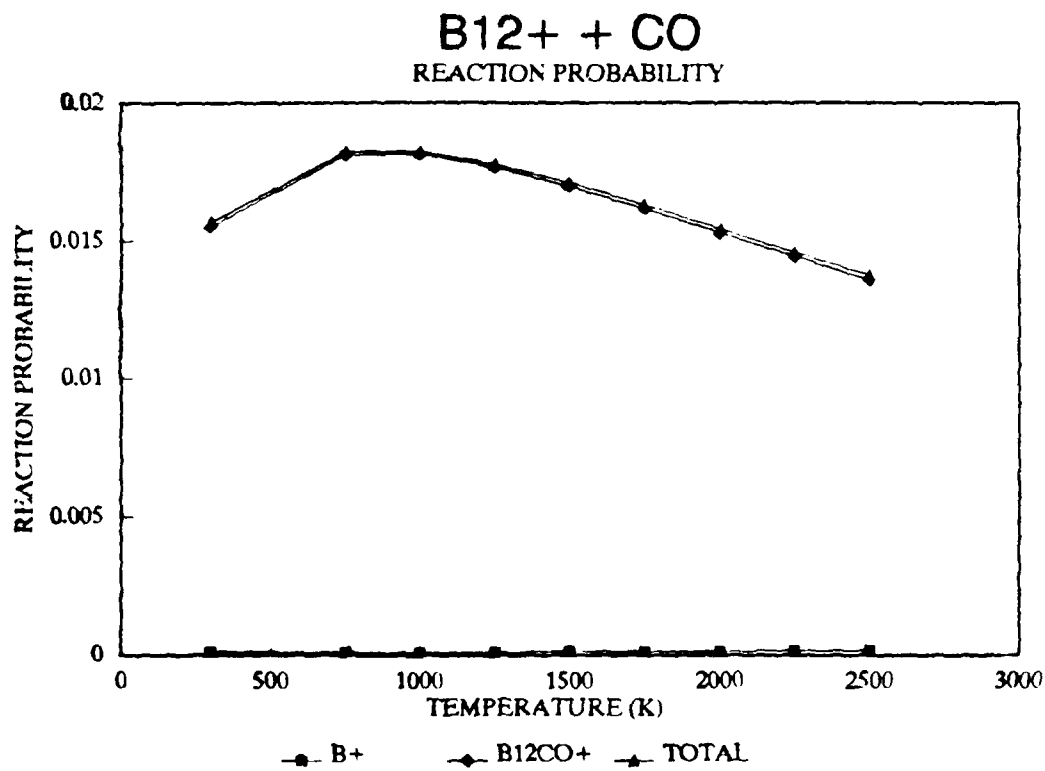
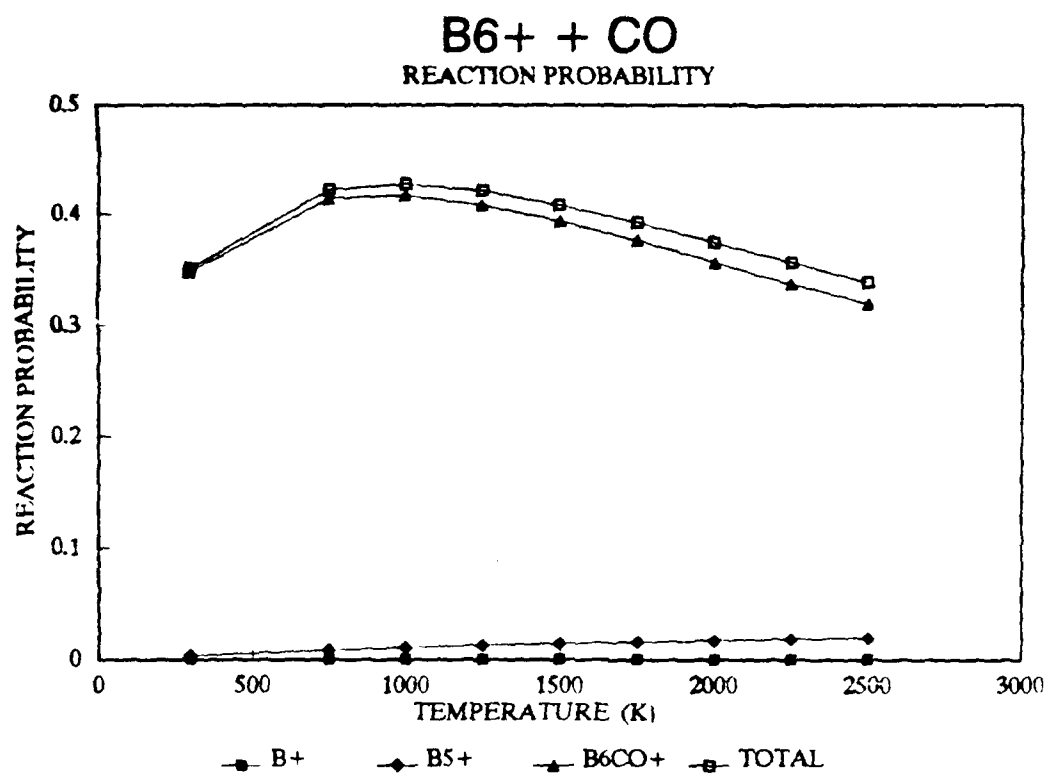


Figure 8

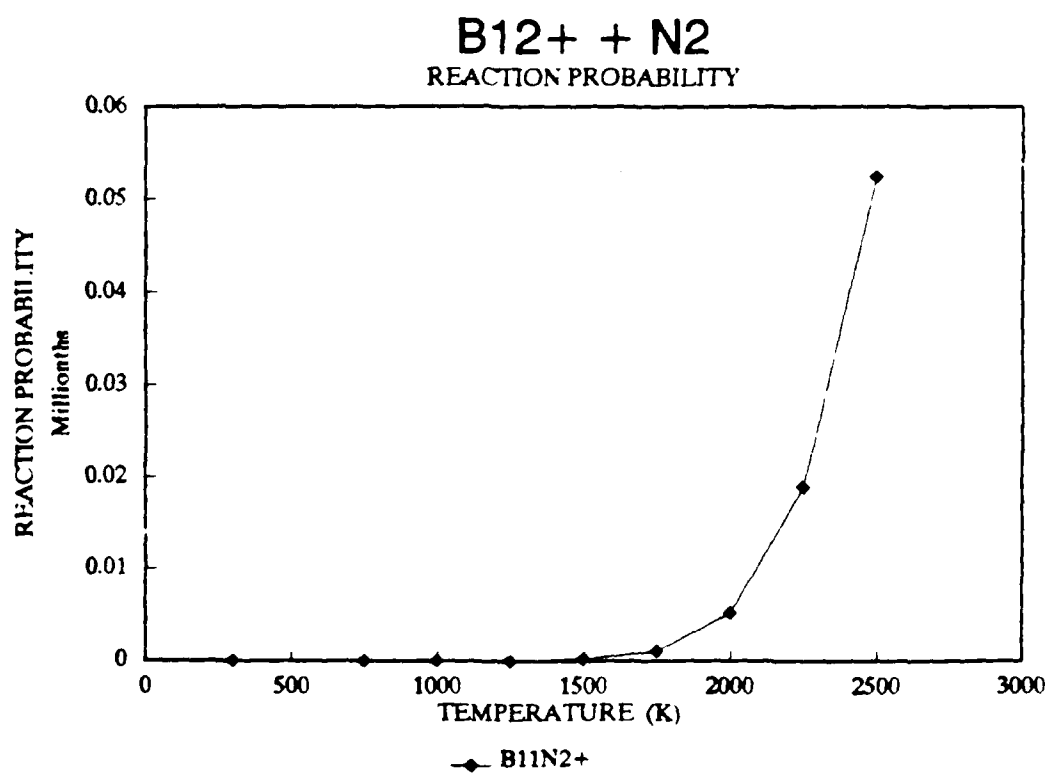
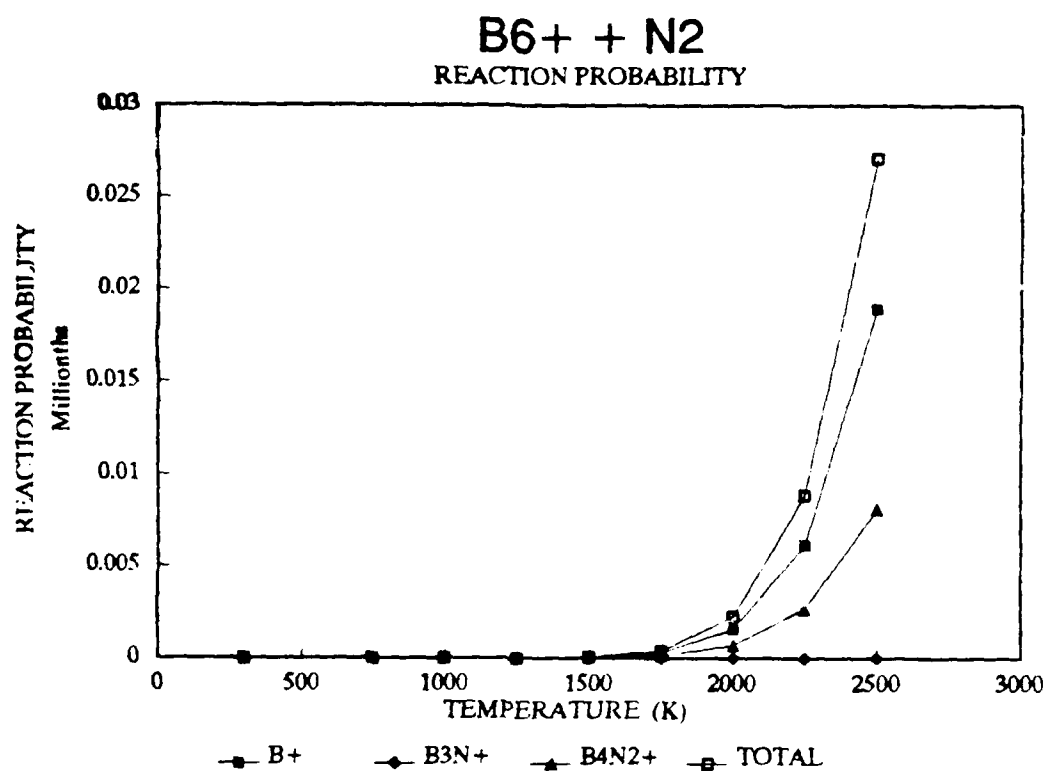


Figure 9

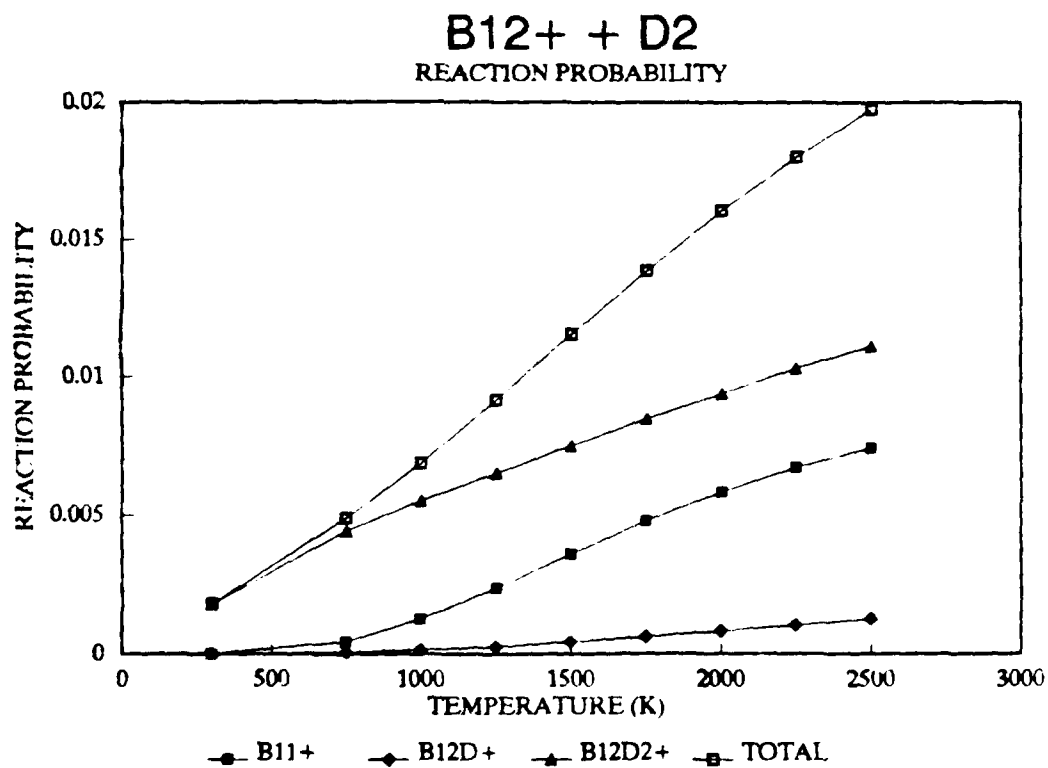
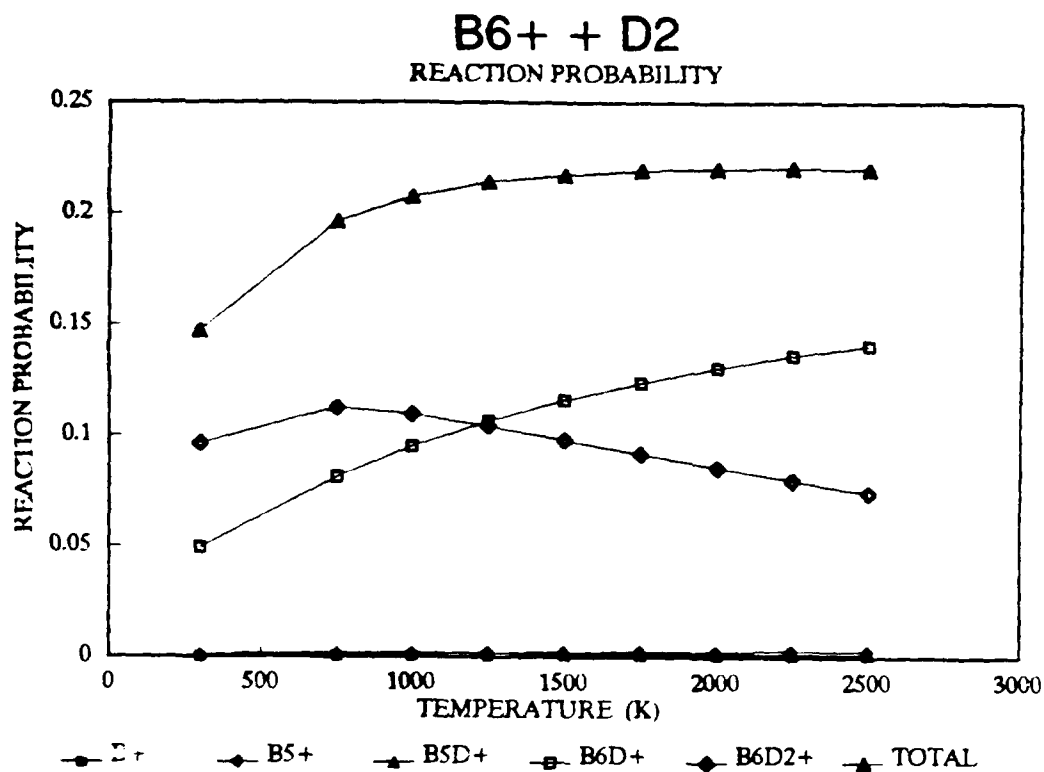


Figure 10

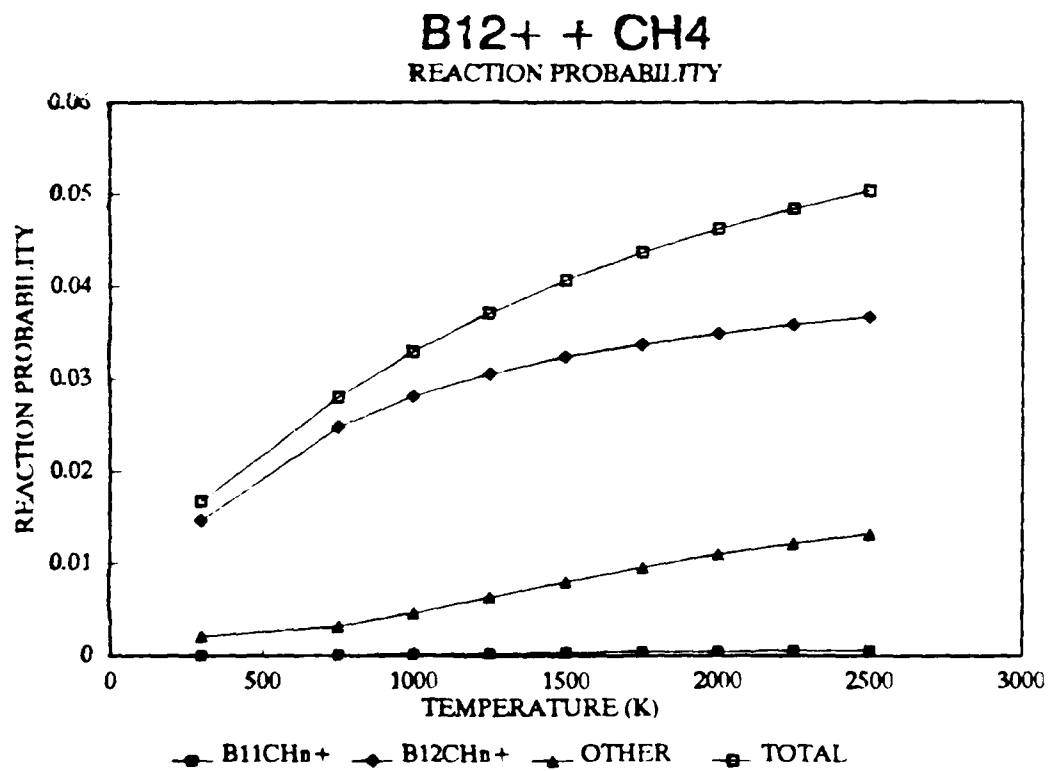
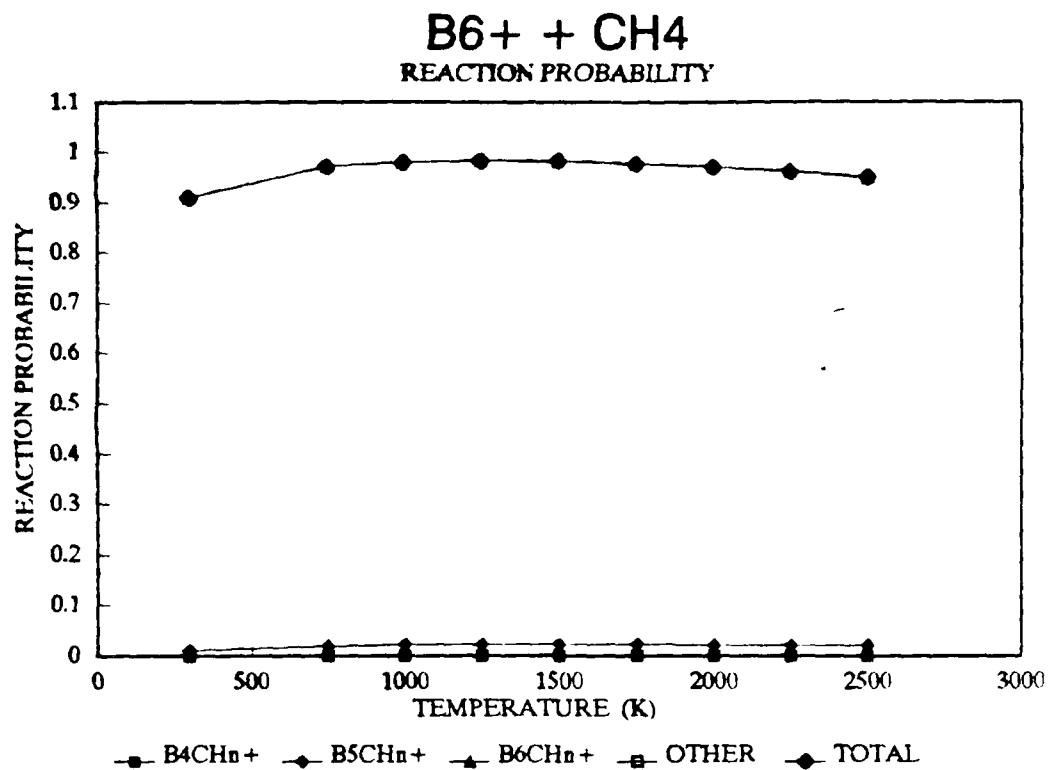


Figure 11

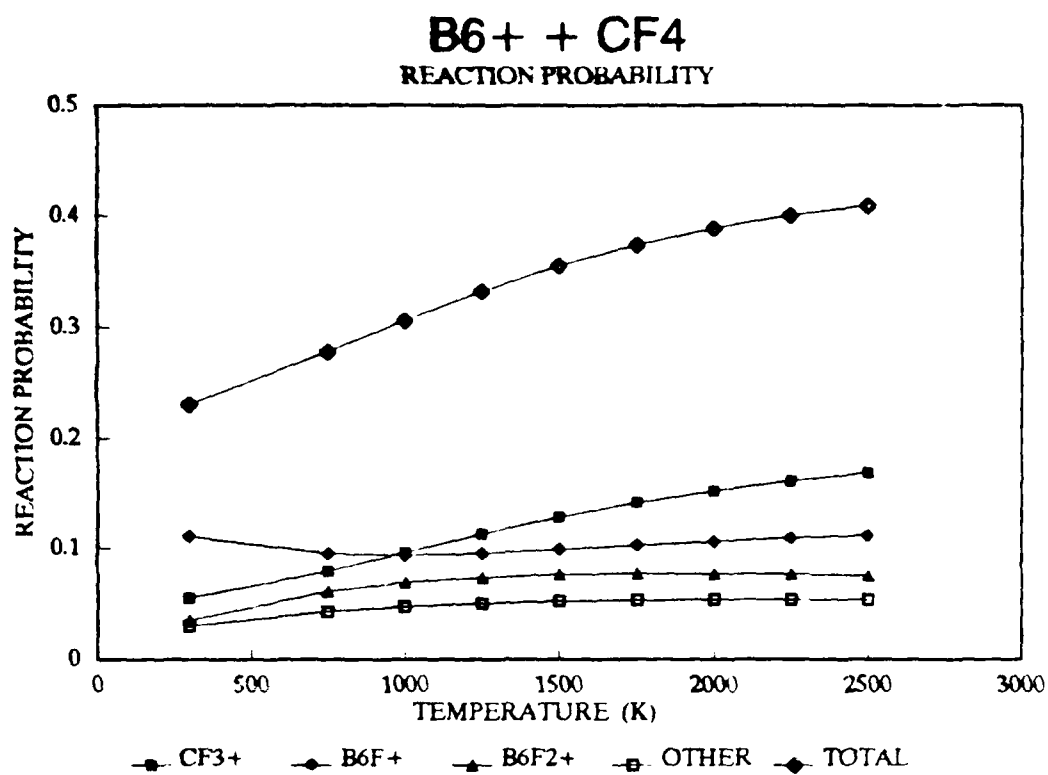


Figure 12

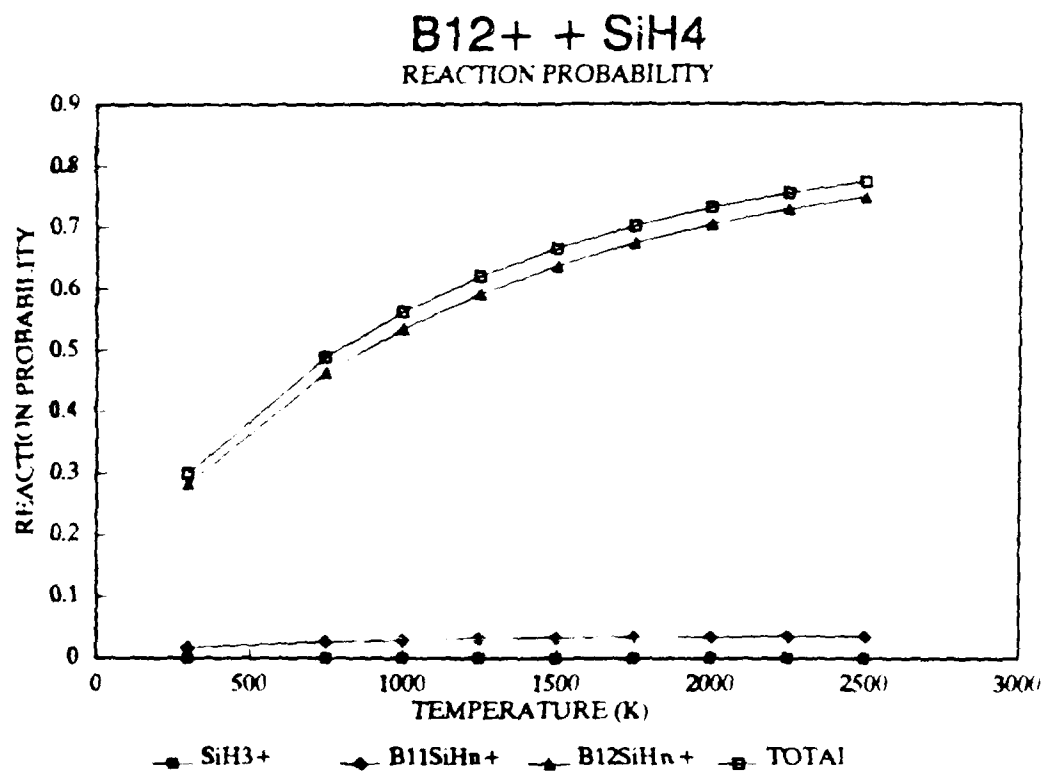
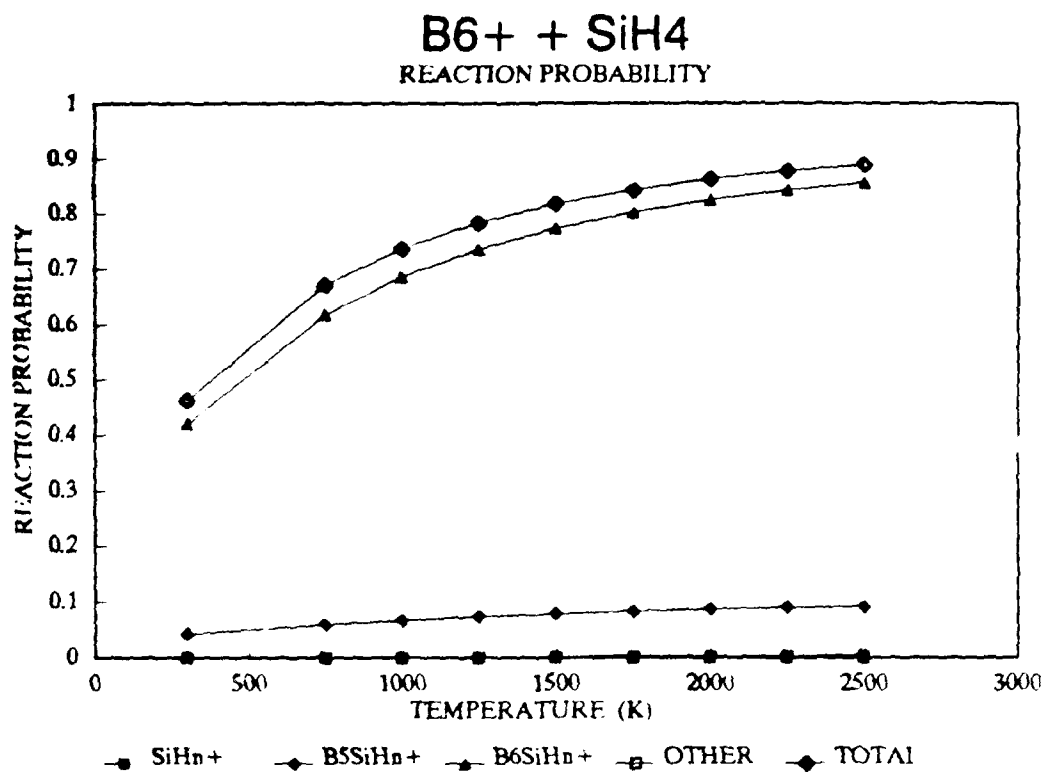
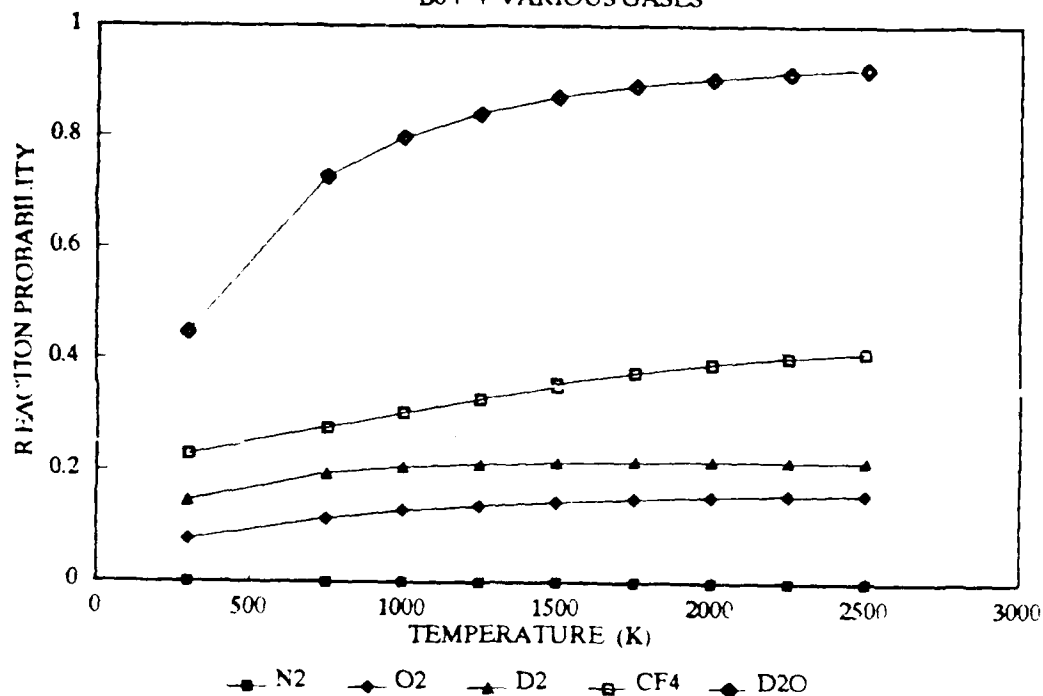


Figure 13

TOTAL REACTION PROBABILITY

B6+ + VARIOUS GASES



TOTAL REACTION PROBABILITY

B6+ + VARIOUS GASES

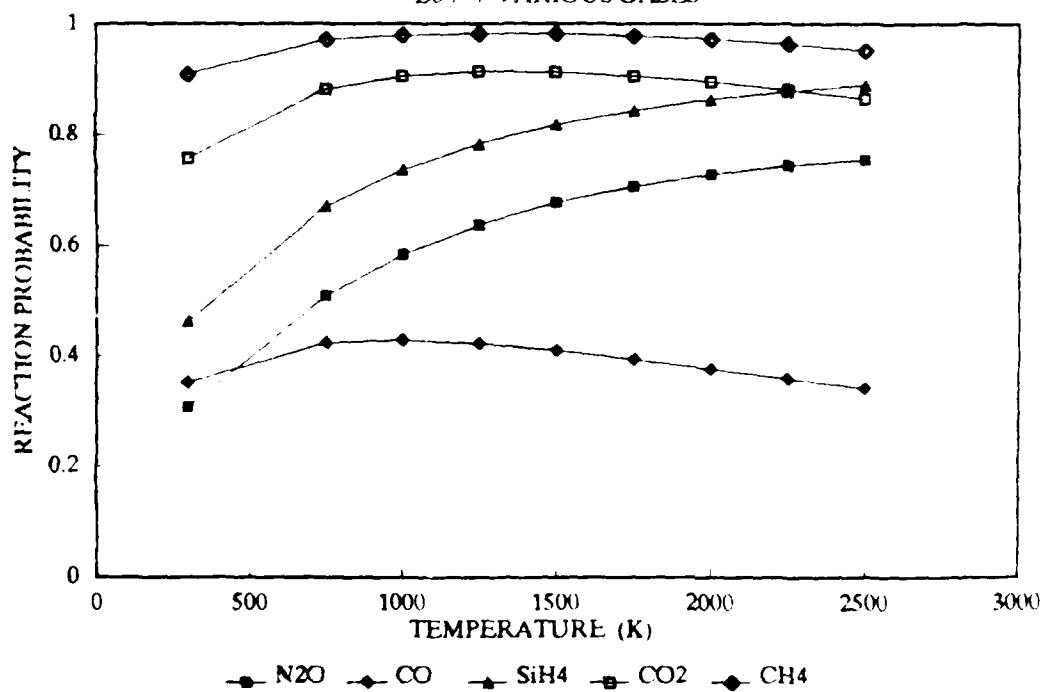
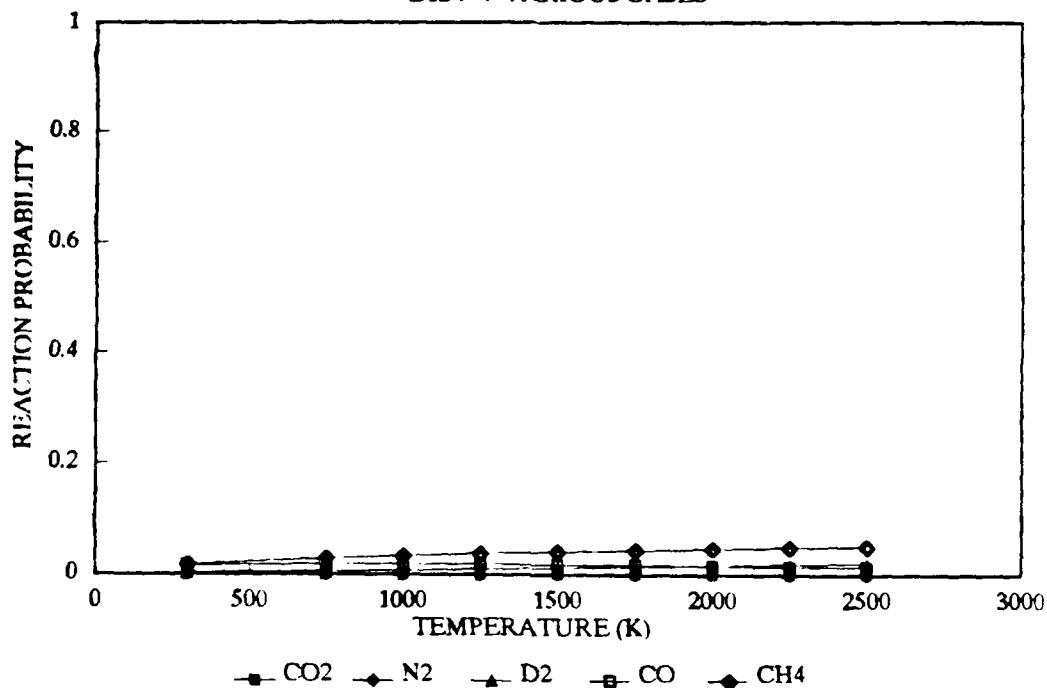


Figure 14

TOTAL REACTION PROBABILITY

B12+ + VARIOUS GASES



TOTAL REACTION PROBABILITY

B12+ + VARIOUS GASES

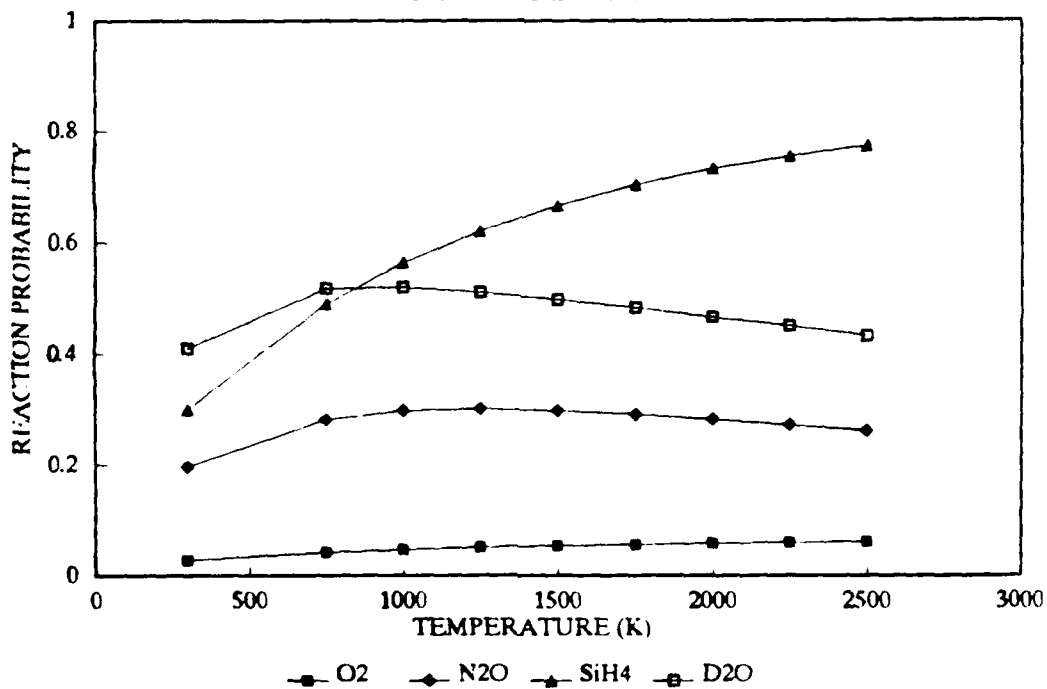


Figure 15